Істотний вплив на точність обробки виробу і продуктивність процесу профільного шліфування надає електроерозійна правка круга.

Для ефективного управління точністю обробки найбільш істотне значення має похибка, викликана зносом алмазного круга. Правку круга необхідно виробляти, коли знос підходить до границі, але не виходить за межі поля допуску. Це дозволить скоротити кількість браку при обробці і скоротити витрату алмазів. Крім того, при цьому скорочується час правки і відповідно підвищується ефективність профільного алмазного шліфування.

Наведено методику та результати експериментальних досліджень зносу профільних алмазних кругів. Дослідження питомої витрати алмазів виконувалися на шліфувальних кругах прямого профілю. Вимірювання величини лінійного зносу круга вироблялося безконтактним методом за допомогою спеціального приладу, заснованого на застосуванні струмовихровий датчиків. Після цього визначалася інтегральна величина зношеного обсягу алмазоносного шару, а потім маса витрачених алмазів. Маса зішліфованого матеріалу визначалася шляхом зважування до і після обробки.

Для встановлення функціональної залежності питомої витрати алмазів від технологічних режимів обробки і параметрів алмазовмісного шару використовувався математичний метод планування і аналізу експериментів. В результаті регресійного аналізу була отримана функціональна залежність питомої витрати алмазу від наступних факторів: концентрації алмазів в крузі, зернистості інструменту, швидкості шліфувального круга, глибини шліфування і швидкості виробу.

Для визначення закономірностей зносу фасонного алмазного круга отримували відбиток його профілю на контрольній пластині з твердого сплаву і вимірювали координати точок робочої частини профілю щодо непрацюючих ділянок. Визначаючи різницю координат до і після досвіду, знаходили величину радіального зносу шліфувального круга у відповідній точці профілю

Ключові слова: профільне шліфування, питома витрата алмазів, технологічні режими обробки, характеристики круга

UDC 621.923
DOI: 10.15587/1729-4061.2020.203685

REVEALING PATTERNS IN THE WEAR OF PROFILE DIAMOND WHEELS

R. Strelchuk
PhD*
E-mail: r.m.strelchuk@gmail.com
S. Trokhymchuk
PhD*
E-mail: trohimchuk_sn@uipa.edu.ua
M. Sofronova
PhD
Department of Power Engineering, Engineering and Physics and Mathematics
Kharkiv State University of Food Technology and Trade
Klochkivska str., 333, Kharkiv, Ukraine, 61051
E-mail: m_myravyova@ukr.net
T. Osypova
PhD
Department of Machine Building and Transport**
E-mail: tanya_338@gmail.com
*Department of Information Computer Technologies and Mathematics**
**Ukrainian Engineering Pedagogics Academy
Universitetska str., 16, Kharkiv, Ukraine, 61003

Received date 18.02.2020
Accepted date 19.05.2020
Published date 19.06.2020

1. Introduction

In today's conditions, competitiveness in machine building is determined primarily by the quality of articles. The most acute issue related to product quality is the manufacture of components of complex configuration from hard-to-treat materials, among which a special place belongs to solid alloys.

Various industries widely use articles with a complex surface configuration. They are made from hard-to-process materials such as solid alloys, ceramics, magnetic alloys, ferrites, etc.

Improvements in the production technology of diamond tools have created real prerequisites for the industrial introduction of the processes of profiled diamond grinding.

We highlight the following scope of application of profiled diamond wheels: machining the shaped solid-alloy cutting and measuring tools, machining basic production articles (non-tool), made from hard-to-process materials, and having a complex shape, as well as the dressing of abrasive tools.

The introduction of profiled diamond grinding to tool production is especially promising.

It is known that the shaped cutting and measuring tools are the most labor-intensive of the entire range of products in tool production, and its use increases due to the high durability of sizes by profile. The use of plunge grinding by a profiled diamond wheel made it possible to reduce the time of manufacture of shaped carbide cutting tools, while eliminating the need for manual refinement, and the durability of cutters increased by 2...2.5 times.

The profiled diamond tools can be widely used in the manufacture of solid alloy stamps, carbide collets, landing tools, solid-alloy carving rollers, tags, rollers, and other tools equipped with a solid alloy.

In the manufacture of solid-alloy monolithic drills and other end tools, profile grinding has been commonly used for the grinding of grooves. Practice shows that when backing up the rear surface of shaped carbide cutters and broaches, profile diamond grinding is the only acceptable technological process.

Given this, it is a relevant field of research to improve the technology of dressing and to devise, based on it, recommendations to improve the efficiency of operations of the profile diamond grinding.

2. Literature review and problem statement

The electroerosive method is the most effective and versatile one for dressing the diamond wheels on metal bundles with complex geometries of the working surface [1]. Our analysis has revealed that the grinding wheel dressing conditions have a significant impact on the technological performance of the profile grinding process and are, therefore, an important controlling factor in the grinding operations [2]. However, the issues related to ensuring the required accuracy and improving the measured durability of profile diamond grinding wheels under conditions of electroerosive dressing are still unresolved. There are no scientifically sound practical recommendations to improve the technology of dressing diamond grinding wheels by electroerosive method.

Paper [3] reports the results of studying the grinding of shaped surfaces. It is shown that in line with this technique for grinding shaped surfaces the profile of an article of any complexity is split into separate sections, which are the arcs of circles and the segments of straight lines. Each section is machined by a diamond wheel of the simplest shape (cylindrical, conical, etc.). The number of tools that work consistently depends on the complexity of the article profile configuration. This grinding technique for shaped surfaces is low-efficient. The reason for this may be the cost of technological and support time, which makes the appropriate technique time-consuming and low-productive. In addition, it is much more difficult to ensure high machining accuracy when it is used due to the need to reinstall wheels.

An option to overcome the related difficulties could be a grinding technique for the shaped face of an article, which involves a profiled diamond wheel whose profile is a mirror image of the profile of the finished article. Unlike the previous technique, this case implies the simultaneous machining of all sections of the profile.

This approach was used in work [4], which shows the use of profiled diamond-abrasive tools made from super-hard materials (diamond, cubic boron nitride). The application of profiled diamond-abrasive tools made from super-hard materials made it possible to develop highly efficient grinding processes employed in various industries.

The use of profile wheels with a diameter of 350 mm and a height of 15 mm when grinding carbide taps for passage increased the machining performance by 5...8 times [5]. The wheel resistance between dressings increased by almost 10 times compared to diamond single-thread wheels.

The interconnected issues of increasing the size stability of profile diamond grinding wheels and active control over the geometry of the grinding tool's work surface at machining were not considered [6].

There are no recommendations to determine the necessary frequency of dressing of profile diamond grinding wheels in the machining of complex-shaped articles, and there are no systemic principles for tackling the issues of targeted modernization of grinding machines.

Thus, there is no single approach to solving individual issues to ensure the accuracy and effectiveness of profile diamond grinding.

The contradictory nature of data available in the literature [7, 8], their fragmented character, and, in some cases, the lack of the required information, leads to the need for comprehensive theoretical and experimental studies. These studies could enhance the technological capabilities of the profile diamond grinding in terms of accuracy and efficiency in the machining of articles of complex configuration.

All this suggests that it is appropriate to conduct a study into the wear of the profiled diamond wheels. In addition, in the course of the study, it is necessary to determine ways to improve the accuracy and performance of the profile diamond grinding by revealing the main patterns of wear of the wheel.

3. The aim and objectives of the study

The aim of this study is to establish patterns of wear of the profile diamond wheel during machining and forming of its work surface at electroerosive dressing. This would provide an opportunity to improve the accuracy and performance of the profile diamond grinding.

To achieve this goal, the following task was solved:

– to investigate the impact of the technological grinding modes and the parameters of a diamond-containing layer of the tool on the specific wheel utilization.

4. Research methods and materials

Experimental studies were carried out at a special bench, based on the surface grinding machine 3E711V, which was modernized by ensuring the slow rotation of the diamond wheel, using interchangeable pulleys, and installing a device for wheel dressing.

We measured the linear wear of the diamond wheel using an eddy current sensor system in the following way [9]. The end of the dielectric tip of the eddy current sensor (ECS) hosts an inductivity coil (Fig. 1).

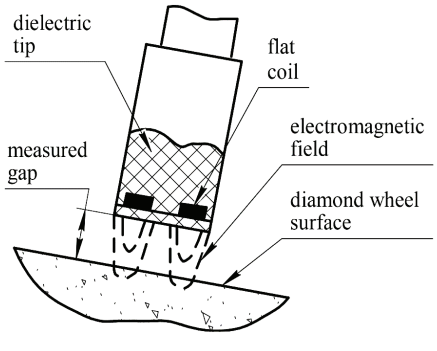

Fig. 1. Schematic of an eddy current sensor

The generator enables the excitation of electromagnetic oscillations in the coil, resulting in an electromagnetic field. In turn, the field interacts with the material of the controlled object; eddy currents are induced at its surface, which change the coil parameters – its active and inductive resistance. The specified parameters change when a gap between the controlled object and the sensor's end changes. The measurements involved a differential eddy current sensor operating at 30 MHz, powered by a high-frequency generator, and consisting of the measuring and support circuits. It has been established that it is most appropriate to use a coil in the sensor,

which is part of a resonance circuit and has a very weak connection to the contour of the generator. A work point was chosen in the middle of the slope of the resonance curve of the circuit. In the ground state, both circuits were adjusted to the same frequency. The supporting circuit was installed in close proximity to the wheel casing, the measuring circuit – near a diamond layer (Fig. 2). Both contours of the sensor, as well as all radio components in the circuit, were sealed.

Since both circuits of the sensor are in close proximity to the wheel and operate under the same conditions, it was possible to avoid errors associated with the system vibrations, the influence of a lubricating cooling technological environment (LCTE), and temperature deformations. The sensors have small dimensions, are easy to handle, and easily installed on the machine.

The sensors were adjusted by a constant voltage supply to two counter-enabled varicaps, connected in parallel to the contour capacitor. The high-frequency voltage that occurs on the contour after detection was amplified and fed to the computer's analog-digital converter (ADC) (Fig. 3). Thus, the output voltage was used to estimate the gap between the end of the measuring circuit sensor and the wheel.

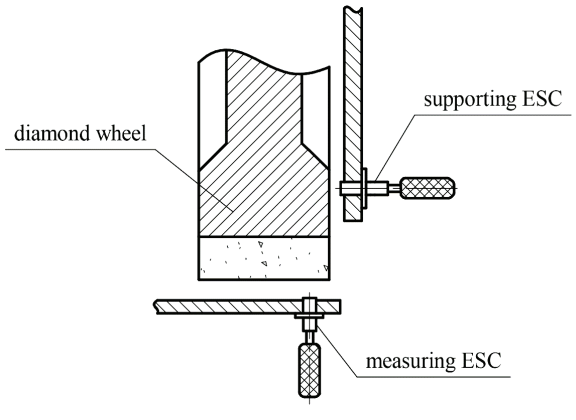

Fig. 2. Contactless measurement scheme of the diamond wheel linear wear

Changing the size of the gap between the sensor and the wheel before the article is machined and after machining makes it possible to determine the amount of wear.

The eddy current sensor system was calibrated by a special device (Fig. 4), which makes it possible to change the size of the gap with high accuracy. The calibration showed that a change in the gap alters the output signal non-linearly, but work along the linear section of the chart makes it possible to register a change in the gap within 0...150 μm with an accuracy of ±3 μm. In this case, the voltage of the output signal changed by 8 mV while increasing the gap between the end of the sensor and the surface of the diamond grinding wheel by 1 μm.

A device was developed to register the wear of the wheel using the MATLAB software package; the device structural diagram is shown in Fig. 5 [10].

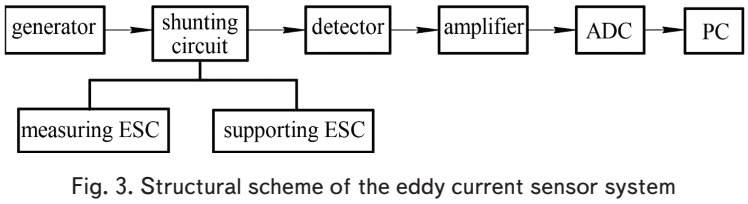

Fig. 3. Structural scheme of the eddy current sensor system

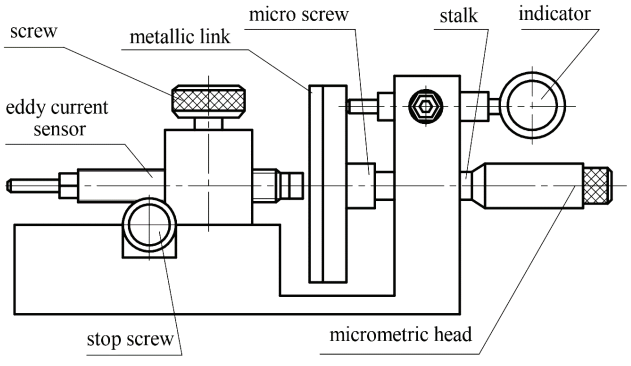

Fig. 4. Schematic of the device for calibrating an eddy current sensor

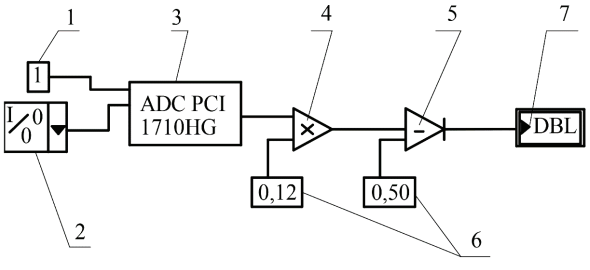

Fig. 5. Structural diagram of the device to register the wear of the wheel: 1 – the number of the device assigned to the I/O board; 2 – analog data entry channel; 3 – I/O board (ADC); 4 – multiplication unit; 5 – subtraction unit; 6 – constant formation unit; 7 – device front panel

The analog signal from analog data entry channel 2 enters the I/O board (ADC) 3, where it is digitalized. The numerical value corresponding to the analog signal is then fed to unit 4, where it is multiplied by the number that establishes the ratio between gap and voltage. Next, the starting gap value corresponding to the wheel zero wear Δ_r is deducted from the resulting value in unit 5. The value of the linear wear of the diamond wheel at a given time, which is registered on device front panel 7, is then determined.

The scale of device 7 is graded in units of wear measure – in micrometers.

The volume of the worn part of the diamond layer was determined from:

$$V_1 = \pi D_k H \Delta_r, \quad (1)$$

where D_k is the diameter of a diamond wheel, mm, H is the width of a diamond wheel, mm (Fig. 6).

The specific utilization of diamonds was calculated from the following formula:

$$q_m = \frac{0.878 V_1}{\alpha_k Q_M}, \quad (2)$$

where α_k is the factor that takes into consideration the concentration of diamonds in a layer; Q_M is the mass of sanded material, g.

The mass of the sanded material was determined by weighing (on analytical scales with an accuracy of 0.1 mg) the diamond grinding wheel before and after machining.

We studied the specific utilization on the sections of the profile of small curvature radii at the

flat inset grinding of samples made from the hard alloy T15K6 by the diamond wheels 14EE1 250×6×76×5 of different characteristics with profile angle φ=60°. The machining was carried out at a depth of grinding (mortise feed) t=0.05 mm.

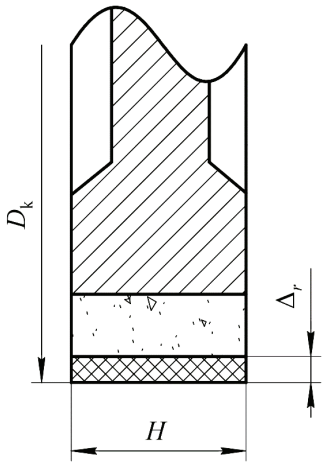

Fig. 6. Schematic of determining the specific utilization of diamonds in a grinding wheel

To determine the volume of the worn part of the diamond-containing layer V_a, we shall conduct mathematical modeling.

Assume that before machining the diameter of the grinding wheel is equal to D_k, the profile angle φ, the radius of the top rounding before machining – r, and after machining – R (Fig. 7).

The volume of the worn part of the diamond-containing wheel layer will be equal to:

$$V_a = \pi D_{k1} F_1, \tag{3}$$

where D_{k1} is the diameter of the grinding wheel after wear, mm; F_1 is the area of the worn part of the wheel in the axial cross-section.

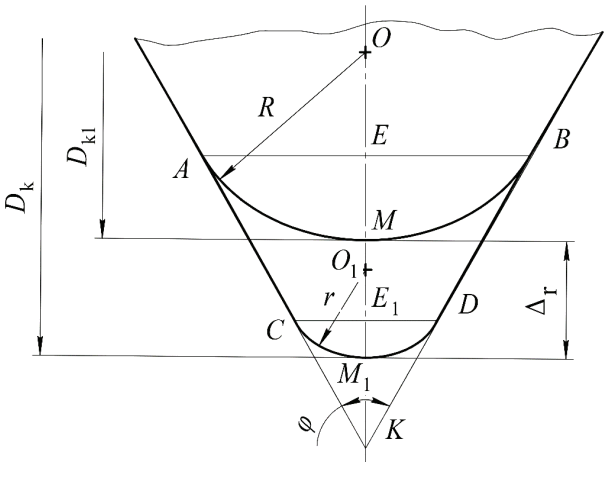

Fig. 7. Schematic of calculating the volume of the worn part of the wheel

The area of the worn part of the diamond-containing layer is equal to the algebraic sum of the trapeze $ABCD$ areas and the segments formed by r and R radii:

$$F_1 = F_{ABCD} + F_r - F_R. \tag{4}$$

After mathematical transformations, the AB and CD segments are equal to, respectively:

$$AB = 2R\cos\frac{\varphi}{2}; \tag{5}$$

$$CD = 2r\cos\frac{\varphi}{2}. \tag{6}$$

The height h of the $ABCD$ trapeze can be found from:

$$h = OK - OE - O_1K + O_1E_1 = \frac{R}{\sin\frac{\varphi}{2}} -$$

$$- \frac{r}{\sin\frac{\varphi}{2}} - R\sin\frac{\varphi}{2} + r\sin\frac{\varphi}{2} = \frac{(R-r)\cos^2\frac{\varphi}{2}}{\sin\frac{\varphi}{2}}. \tag{7}$$

The $ABCD$ trapeze area is determined as follows:

$$F_{ABCD} = \frac{AB+CD}{2}h = \frac{\left(R^2 - r^2\right)\cos^3\frac{\varphi}{2}}{\sin\frac{\varphi}{2}}. \tag{8}$$

The areas of the segments formed by r and R radii are equal to, respectively:

$$F_r = \frac{r^2}{2}\left(\frac{\pi}{180}\varphi - \sin\varphi\right); \tag{9}$$

$$F_R = \frac{R^2}{2}\left(\frac{\pi}{180}\varphi - \sin\varphi\right). \tag{10}$$

By substituting the values F_{ABCD}, F_r and F_R into expression (4), we obtain:

$$F_1 = \left(R^2 - r^2\right)\left(\operatorname{ctg}\frac{\varphi}{2} - \frac{\pi}{360}\varphi\right). \tag{11}$$

The diameter of the grinding wheel changes during the machining process due to the wear of the top. Assume that the linear amount of the top wear is equal to Δ_r.

The size of the OK segment can be expressed as:

$$OK = OM + MM_1 + M_1K. \tag{12}$$

We find from ΔO_1CK:

$$O_1K = \frac{r}{\sin\frac{\varphi}{2}}. \tag{13}$$

The M_1K segment is determined from:

$$M_1K = O_1K - O_1M_1 = r\left(\frac{1}{\sin\frac{\varphi}{2}} - 1\right). \tag{14}$$

Substituting (14) into (12) and taking into consideration that OM=R and MM_1=Δ_r, we obtain:

$$OK = R + \Delta_r + r\left(\frac{1}{\sin\frac{\varphi}{2}} - 1\right). \quad (15)$$

On the other hand, we have from ΔOAK:

$$OK = \frac{R}{\sin\frac{\varphi}{2}}. \quad (16)$$

By equating (15) and (16) and solving the resulting equation relative to Δ_r, we find:

$$\Delta_r = (R - r)\left(\frac{1}{\sin\frac{\varphi}{2}} - 1\right). \quad (17)$$

The diameter of the grinding wheel after wear is determined as:

$$D_{k1} = D_k - 2\Delta_r. \quad (18)$$

We obtain, by substituting (17) into (18):

$$D_{k1} = D_k - 2(R - r)\left(\frac{1}{\sin\frac{\varphi}{2}} - 1\right). \quad (19)$$

Taking into consideration (19), expression (3) to determine the volume of the worn part of the diamond-containing layer can finally be written in the following form:

$$V_a = \pi\left[D_k - 2(R-r)\times\left(\frac{1}{\sin\frac{\varphi}{2}} - 1\right)\right]\times \times (R^2 - r^2)\left(\operatorname{ctg}\frac{\varphi}{2} - \frac{\pi}{360}\varphi\right). \quad (20)$$

We measured the radius of the diamond grinding wheel top rounding before and after machining at the tool microscope BMI-1c after receiving a replica on the control plate made from a solid alloy.

The specific utilization of diamonds was calculated from formula (2).

A diamond wheel was used to study the wear of the grinding wheels of the shaped profile; its profile is represented by the circumference arc (Fig. 8). The wheel was profiled by electroerosive method and was used for 20 minutes to remove loosely fixed and poorly oriented grains. The diamond wheel then crashed into a solid alloy control plate to a depth of 3 mm to obtain a replica of the original profile of the work surface.

The specified wheel was then used to polish the samples made from the solid alloy T15K6, the dimensions of 20×20×150 mm, with a pre-prepared profile. That provided the same working conditions for different sections of the work surface. Samples were mounted parallel to the table path in a vise. After machining the required number of samples, we received a replica of the profile of the worn surface of the diamond wheel.

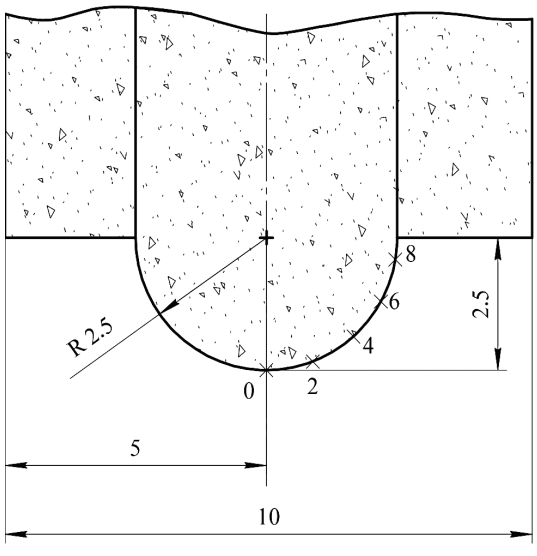

Fig. 8. Configuration of the profile of the shaped diamond wheel

In order to acquire data on the nature of the wheel wear at various sites, the tool microscope BMI-C was used to measure the coordinates of points 0...8 of the profile relative to the non-utilized sections *A* and *B* (Fig. 9). The amount of radial wear Δ_{ri} at the relevant profile point was found as a difference between the h_{iH} and h_{iK} coordinates before and after grinding.

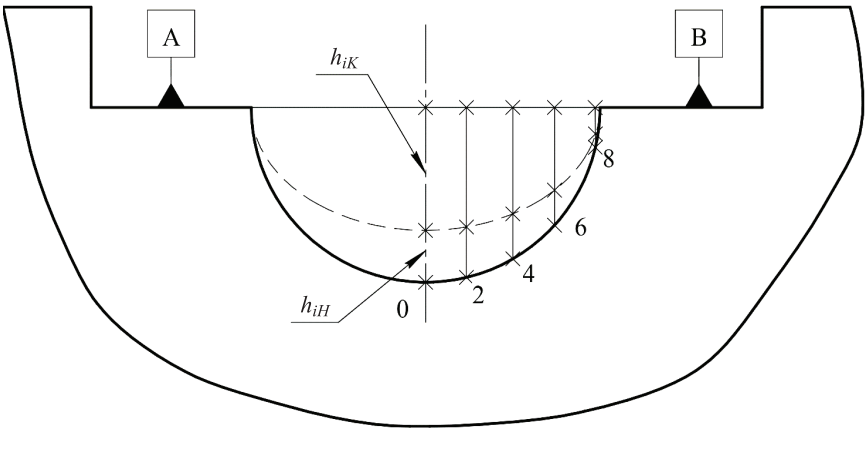

Fig. 9. Schematic of determining the linear radial wear of a diamond grinding wheel

5. Studying the impact of the technological modes of grinding and the parameters of a diamond-containing layer of the tool on the specific wheel utilization

A method of planning experiments was used to derive the functional dependence of the diamond wheel specific utilization q_m on the technological machining modes and the parameters of a diamond-containing layer of the tool. Based on qualitative analysis and the results of preliminary experiments, we chose the following factors for the construction of a mathematical model: *K* is the concentration of diamonds

in a wheel; Z is the grit of diamond wheels, μm; V_k is the grinding wheel velocity, m/s; t is the depth of grinding, mm; V is the article speed, m/min. The levels and intervals of variation of the examined factors are given in Table 1.

Table 1

Levels and intervals of factor variation

Natural factor designation	K	Z, μm	V_k, m/s	t, mm	V, m/min
Factor encoded designation	X_1	X_2	X_3	X_4	X_5
Upper level	6 (150 %)	200 (160/125)	35	0.125	16
Bottom level	2 (50 %)	40 (50/40)	15	0.025	2
Basic level	4 (100 %)	120 (100/80)	25	0.075	9
Variation interval	2 (50 %)	80	10	0.05	7

In order to derive a power dependence, the transformation of the optimization parameter by logarithm was performed.

The encoded factors were used instead of their natural values to make it easier to write down the conditions of the experiment and process the data obtained. The encoding was performed using the following ratio:

$$X_i = \frac{2\left(\ln x_i - \ln x_{\max}\right)}{\ln x_{i\max} - \ln x_{i\min}} + 1, \quad (21)$$

where $x_{i\max}$, $x_{i\min}$ are, respectively, the values of factors at the upper and lower levels.

Given the laborious implementation of the full factor experiment, a fractional factor experiment of the 2^{5-1} type was used, that is, a half-replica of the full factor 2^5 plan, set by the generating ratio:

$$X_5 = X_1X_2X_3X_4.$$

In this case, the defining contrast takes the form:

$$I = X_1X_2X_3X_4X_5.$$

The ratios that set the joint estimates of regression coefficients were found by the multiplication of the defining contrast consistently by X_1, X_2, etc. The analysis showed that in this case, none of the linear effects mixes with the pair interaction, but is estimated together with the interaction of higher orders. Therefore, the resolution of the selected fractional replica is the maximum possible. The planning matrix and the results of the experiments are given in Table 2.

The experiments were conducted in a random sequence according to data in Table of the evenly distributed random numbers. Experiments were repeated three times in each experiment. Table 2 gives the average value of the diamond wheel specific utilization $\overline{q}_m$.

The result of the mathematical treatment of the data is the determined regression coefficients. The comparison of absolute values of the regression coefficients with the size of the confidence interval showed that the statistically significant coefficients were b_1, b_2, b_3, b_4, b_5.

The hypothesis about the adequacy of the model was tested by Fisher's criterion:

$$F = \frac{S_{ad}^2}{S_y^2}, \quad (22)$$

where S_{ad}^2 is the variance of adequacy; S_y^2 is the variance of reproducibility.

The variance of adequacy S_{ad}^2 was calculated from the following formula:

$$S_{ad}^2 = \frac{\sum_1^N n\left(\overline{y} - \widehat{y}\right)^2}{N - \lambda}, \quad (23)$$

where $\overline{y}$ is the average value of a single observation, $\widehat{y}$ is the estimated value of a criterion based on the regression equation, n is the number of repetitions of a given experiment, N is the total number of experiments, λ is the number of equation coefficients.

The variance of reproducibility S_y^2 is determined from the following expression:

$$S_2^y = \frac{\sum_1^N \sum_1^n \left(y_{uj} - \overline{y}_u\right)^2}{N\left(n-1\right)}, \quad (24)$$

where N is the total number of experiments, n is the number of repetitions of a given experiment; y_{uj} are the results of a separate observation; $\overline{y}_u$ is the arithmetic mean value of the criterion.

Table 2

Planning matrix and experiment results

Experiment No.	X_1	X_2	X_3	X_4	X_5	Specific diamond wheel utilization $\overline{q}_m$, mg/g
1	2	40	15	0.025	16	0.735
2	6	40	15	0.025	2	0.195
3	2	200	15	0.025	2	0.085
4	6	200	15	0.025	16	0.160
5	2	40	35	0.025	2	0.240
6	6	40	35	0.025	16	0.360
7	2	200	35	0.025	16	0.165
8	6	200	35	0.025	2	0.050
9	2	40	15	0.125	2	1.430
10	6	40	15	0.125	16	2.290
11	2	200	15	0.125	16	1.070
12	6	200	15	0.125	2	0.310
13	2	40	35	0.125	16	2.570
14	6	40	35	0.125	2	0.720
15	2	200	35	0.125	2	0.32
16	6	200	35	0.125	16	0.520

The adequacy of the model was tested based on Fisher's criterion. The F value, found from equation (22), was compared to a tabular one. The estimated value of the criterion was less than the tabular value at a 95 % level of significance, therefore, the resulting equation is adequate.

Thus, the regression equation in the encoded coordinates takes the form:

$$y = -0.93 - 0.19X_1 - 0.59X_2 - 0.14X_3 + 0.78X_4 + 0.44X_5.$$

After decoding and potentiation, we derived the desired functional dependence of the specific diamond utilization on the examined factors:

$$q_m = \frac{t^{0.56}V^{0.44}}{K^{0.27}Z^{0.74}V_k^{0.24}}. \quad (25)$$

The functional dependence shows the level of influence exerted on the specific utilization of diamond wheels by the technological machining modes and the parameters of a diamond-containing layer of the tool.

Fig. 10 shows the graphic dependence of specific utilization on the parameters of a diamond-containing layer. Fig. 10 demonstrates that the increase in the graininess of diamond powder, all other things being equal, causes a decrease in the specific utilization q_m. The increase in the concentration of diamonds in a wheel leads to a decrease in specific utilization q_m.

Among the technological machining modes, the largest impact on the amount of specific utilization is exerted by the depth of grinding (mortise feed). Increased grinding depth leads to an increase in the specific utilization of diamonds (Fig. 11).

The chart, shown in Fig. 11, demonstrates that an increase in the article speed leads to an increase in specific utilization.

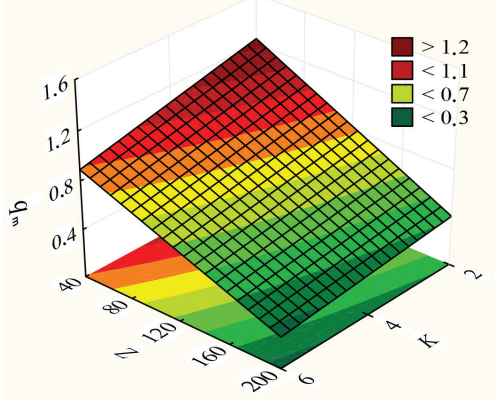

Fig. 10. Response surface $q_m - (Z, K)$. Calculation conditions V_k=25 m/s, t=0.075 mm, V=9 m/min

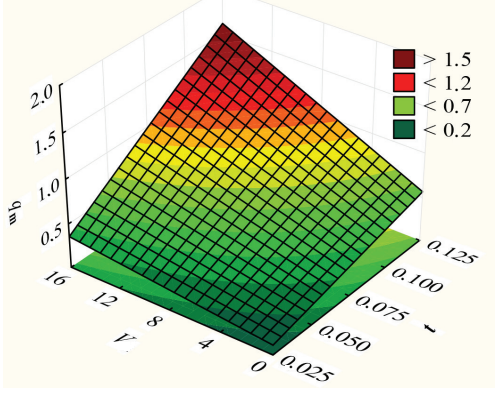

Fig. 11. Response surface $q_m - (V, t)$. Calculation conditions K=4 (100 %), Z=120 (100/80) μm, V_k=25 m/s

Fig. 12 shows the effect of the grinding wheel velocity V_k on the specific utilization of diamonds in a wheel. The chart, shown in Fig. 12, demonstrates that an increase in the grinding wheel velocity leads to a decrease in the specific utilization of diamonds.

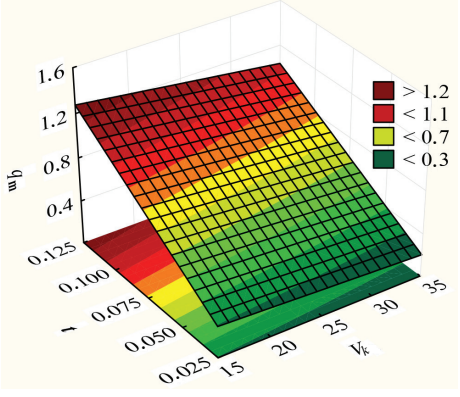

Fig. 12. Response surface $q_m - (V_k, t)$. Calculation conditions K=4 (100 %), Z=120 (100/80) μm, V=9 m/min

6. Discussion of the study results

Fig. 10 shows the graphic dependences of specific utilization on the parameters of a diamond-containing layer. An increase in the graininess of diamond powder causes a decrease in specific utilization q_m. This result can be explained by that the increase in the grain size increases the strength of their fixation in the wheel bundle. The increased concentration of diamonds in a layer leads to an increase in the number of cutting grains. In turn, this leads to a reduction in the load on the grain and, accordingly, to a reduction in the specific utilization of diamonds.

Increased grinding depth leads to an increase in the specific utilization of diamonds (Fig. 11). That increases the thickness of the layer of material removed by a single grain. In this case, the friction forces in the contact area between the wheel and the article vary slightly. Therefore, the change in the article speed has less impact on the specific utilization of diamonds than the change in the depth of grinding.

The chart, shown in Fig. 12, demonstrates that the increase in the grinding wheel velocity decreases the specific utilization of diamonds. This can be explained by a decrease in the time of contact between the wheel and the article, as well as a decrease in the size of the chips removed by diamond grains.

The revealed patterns of wear in the diamond grinding wheels of a complex profile during machining make it possible to predict the precision parameters of the polished article.

We have investigated the effect of technological grinding regimes and machining conditions on the specific utilization of diamonds q_m. As a result of the study, a functional dependence of the specific utilization of diamond wheel q_m on the technological machining conditions and the parameters of a diamond-containing layer has been obtained. The established dependence reflects the impact of the technological grinding modes and the parameters of a diamond-containing layer of the tool on specific utilization. By using this dependence, one can determine the intensity of the wear of the grinding tool.

The limitations of the study are as follows. The variation intervals and the number of factors are set in a specific

range, taking into consideration practical recommendations. The range under study is taken at the stage of the finishing operation in the technological process of grinding an article of a complex configuration with the required precision of machining. The proposed mathematical model to determine the volume of the worn part of a diamond-containing layer produces an adequate result of calculating the specific diamond wheel utilization. The study did not take into consideration factors such as the material being machined, the type of a diamond wheel ligament, and uneven wear at various sections of the tool. These factors could impact the wheel specific utilization.

The caveats of this study include the following. When constructing a mathematical model, the parameters of the generator for electroerosive dressing were not selected as factors. In the future, they can be taken into consideration but, at the same time, the laboriousness of the experiment will increase.

The current study could be advanced by devising recommendations to determine the necessary dressing frequency of profile diamond wheels when machining articles of complex shape. In the future, the study will address the task of designing and developing a device to actively control the geometry of the grinding tool's work surface.

7. Conclusions

We have investigated the effect of the technological modes of grinding and the parameters of a diamond-containing layer of the tool on the specific wheel utilization. The study result is the derived functional dependence of the specific diamond wheel utilization q_m on the technological machining regimes and the parameters of a diamond-containing layer of the tool. The resulting dependence makes it possible to calculate the specific diamond wheel utilization q_m and determine the necessary dressing period for diamond wheels when machining articles of complex shape. Studies of the impact of technological grinding regimes and the parameters of a diamond-containing layer of the tool improve the effectiveness of the profile diamond grinding. The efficiency of the grinding process will be ensured by the required precision when machining articles of complex configuration.

References

1. Zhang, Q., Zhao, Q., To, S., Guo, B., Zhai, W. (2017). Diamond wheel wear mechanism and its impact on the surface generation in parallel diamond grinding of RB-SiC/Si. Diamond and Related Materials, 74, 16–23. doi: https://doi.org/10.1016/j.diamond.2017.01.019
2. Liang, Z. (2018). Experimental Study on Diamond Wheel V-tip Truing Using a Tangential Grinding Truing Method. Journal of Mechanical Engineering, 54 (3), 196. doi: https://doi.org/10.3901/jme.2018.03.196
3. Zverovshikov, V. Z., Sokolov, A. V. (2011). Povyshenie kachestvennyh harakteristik poverhnosti pri profil'nom almaznom shlifovanii. Izvestiya vysshih uchebnyh zavedeniy. Povolzhskiy region. Tehnicheskie nauki, 3 (19), 167–174.
4. Guo, B., Zhao, Q. (2015). On-machine dry electric discharge truing of diamond wheels for micro-structured surfaces grinding. International Journal of Machine Tools and Manufacture, 88, 62–70. doi: https://doi.org/10.1016/j.ijmachtools.2014.09.011
5. Xie, J., Deng, Z. J., Liao, J. Y., Li, N., Zhou, H., Ban, W. X. (2016). Study on a 5-axis precision and mirror grinding of glass freeform surface without on-machine wheel-profile truing. International Journal of Machine Tools and Manufacture, 109, 65–73. doi: https://doi.org/10.1016/j.ijmachtools.2016.07.011
6. Asplund, M., Lin, J. (2016). Evaluating the measurement capability of a wheel profile measurement system by using GR&R. Measurement, 92, 19–27. doi: https://doi.org/10.1016/j.measurement.2016.05.090
7. Wang, Y., Lan, Z., Hou, L., Zhao, H., Zhong, Y. (2015). A precision generating grinding method for face gear using CBN wheel. The International Journal of Advanced Manufacturing Technology, 79 (9-12), 1839–1848. doi: https://doi.org/10.1007/s00170-015-6962-0
8. Márton, L. (2018). About The Modernized Grinding Wheel Dressingdevice S Diamond-Pin Driving System by The Nilesgear Grinding Machines. Műszaki Tudományos Közlemények, 9 (1), 155–158. doi: https://doi.org/10.33894/mtk-2018.09.34
9. Chowdhury, M. A. K. (2015). Grinding Wheel Surface Topography for Multiple Pass With Incremental Depth of Cut of Rotary Diamond Dresser. Volume 2B: Advanced Manufacturing. doi: https://doi.org/10.1115/imece2015-53342
10. Cheng, W. (2012). Pulsed Eddy Current Testing of Carbon Steel Pipes' Wall-thinning Through Insulation and Cladding. Journal of Nondestructive Evaluation, 31 (3), 215–224. doi: https://doi.org/10.1007/s10921-012-0137-9